Application of Stabilized Monodisperse Antimicrobial Silver Nanoparticles Produced from x- ray and Photographic Films as Corrosion Inhibitor for Carbon Steel in Aqueous Acidic Solution

Ayman M. Atta[1,2,], Gamal A. El-Mahdy[1,3], Hamad A. Al-Hodan[1], Abdelrahman O. Ezzat[1]*

[1] Surfactants research chair, Chemistry department, college of science, King Saud University, Riyadh 11451, Saudi Arabia.
[2] Petroleum Application Department, Egyptian Petroleum Research Institute, Nasr City 11727, Cairo, Egypt.
[3] Chemistry department, Faculty of science, Helwan university, Helwan, Egypt.
[*]E-mail: aatta@ksu.edu.sa

New antimicrobial silver nanoparticles (Ag NPs) can be synthesized using recycled X-ray and photographic films by green, simple, easy, cost effective and environment-friendly chemical method. It is based on stripping both Ag^+ ions and gelatin layer of recycled films followed by reducing silver ions in an aqueous media in the absence and presence of glucose and poly(vinylpyrrolidone), PVP, as reducing and stabilizing agents. In this study, gelatin acts as a reducing and stabilizing agent for the first time. The optimum conditions such as stripping time, temperature, gelatin and PVP concentrations, crystalline structure, particle distribution and size of Ag NPs was investigated. Ultraviolet - visible spectra was used to study the chemical stability of Ag NPs in 1M HCl to be applied as a thin antimicrobial layer to protect the steel surface from corrosion.

1. INTRODUCTION

Green chemistry, also known as sustainable chemistry, is used to design, manufacture, and use new chemical substances and processes that reduce or eliminate the use or generation of hazardous substances [1]. Silver nanoparticles, Ag NPs, possess excellent biological activity as antimicrobial and attracted great attentions as nanomaterials having distinctive thermal, optical and electrical properties [2-6]**.**There are different techniques have been widely used to prepare Ag NPs based on reduction

method and toxic organic solvents, reducing agent, and capping agents to increase their stability towards environment[7-10]. This problem was solved by using advanced methods based on biosynthesis and electrochemical techniques that required special efforts and instruments [11-15]. The chemical stability of Ag NPs to different environments and low yield and stabilization were the main drawbacks of these methods. The storage stability of Ag NPs and conversion of silver to silver ions that increase the toxicity of nanoparticles are still unsolved issues. Moreover, great challenges require more efforts to solve such as production monodisperse, size and shape controlled Ag NPs. The main objective of the present work are based on reducing the production cost, control particle size and shapes, and reproducibility Ag NPs.

The production of Ag NPs from wastes such as x-ray medical and photographic films after photo reduction was reported using either electrochemical deposition or chemical reduction method based on hazardous chemicals [16-18]. They failed to solve the several challenges to prepare Ag NPs but they succeeded to reduce the cost and time. In our work, we aim to apply twelve principles of the green chemistry to prepare highly stabilized silver nanoparticles. Moreover, this work reports at first time for preparing Ag NPs having monodisperse, stabilized and small size with controlled shape from silver ion rather than silver nitrate, silver acetoacetate and silver ammonium complexes. In this respect, a simple green way was used for producing silver nanoparticles by reducing silver chloride imbedded with polyester and gelatin of photographic and medical x-ray films, using glucose and poly(vinyl pyrrolidone), PVP, in alkaline media as reducing and capping agents, respectively. Glucose, gelatin and PVP have the ability to reduce silver in better control of the silver particle size and stability. Transmission electron microscopy (TEM), dynamic light scattering (DLS) and UV−vis spectroscopy were employed to characterize the synthesized Ag nanoparticles. The acid resistivity of the produced silver nanoparticles to stomach synthetic fluid (0.4 M HCl; 0.4 M glycine in deionized water) was investigated.

2. EXPERIMENTAL

2.1. Materials

A Fuji medical X-ray and photographic film wastes (having silver content 5 g /m^2) were used as recycled materials. Glucose, poly (vinylpyrrolidone) with molecular mass 40000 g/mol (PVP), ammonia solution 25 % and sodium hydroxide purchased from Aldrich Sigma Co. were all used without purification.

Carbon steel chemical compositions, the method of electrode preparation as working electrode and method of preparation to investigate its corrosion resistance in the presence of 1M HCl and aqueous dispersion solution of Ag NPs used in corrosion test are reported in previous study [19].

2.2. Preparation technique

The waste x-ray and photographic films (10 g) were cut into tiny portions and mixed with 90 mL (25-28 % of ammonia solution) and PVP (2 g). The reaction temperature was increased to 50 ^{o}C

until the colour of solution became blue. Then, the temperature increased to 60 $^{\circ}$C where the colour of solution converted from blue to dark red. The solid film pieces were filtered out. Ag NPs were separated at 15000 rpm of ultracentrifuge. The same procedure repeated and 90 mL (1 M NaOH solution) was used instead ammonia solution. Ag NPs can also be prepared from x-ray film wastes in the presence of same reagents beside 10 mL aqueous solution (contains 4 g of glucose) added to the reaction mixture. The temperature was raised up slowly up to 90 $^{\circ}$C during a period of 1 hr. The red color of reaction mixture was converted to black. Silver nanoparticles were separated at 21000 rpm of ultracentrifuge.

2.3. Characterization

UV-Vis spectrophotometer (UV-2450, Shimadzu, Kyoto, Japan) was used to confirm the formation of Ag NPs and their stability in 1M HCl aqueous solution from its surface plasmon absorption band.

The size distribution and dispersion of Ag NPs were characterized by a nanoparticle size analyzer 3000HS PCS (Malvern Instruments).

The morphology of the Ag NPs was elucidated using a high-resolution transmission electron microscopy (HR-TEM; JEOL JEM-2100F).

The XRD patterns were carried out on Philips (X'Pert, Philips, Netherlands, Cu Kα radiation of wavelength 1.54 Å) and recorded at a scan speed of 2°/min.

The atomic force microscope (AFM) image was recorded on an Ambios Q-scope® (Ambios Technology, Santa Cruz, CA, USA) (SPM) machine.

Size distribution and zeta potential of the magnetic nanogel were determined by a Zetasizer 3000HS PCS (Malvern Instruments).

2.4. Antimicrobial and Bactericidal Assays

Antimicrobial performance of the prepared silver colloid was assessed using the standard dilution micromethod as illustrated in previous work [20]. After 24 h of incubation at 37 °C, the minimum inhibitory concentration (MIC) was recorded as the MIC of the tested material that inhibit the outgrowth of the bacterial strain.

2.5. Electrochemical measurements

The electrochemical behaviors of AgNPs were evaluated in 1 M HCl aqueous solution from electrochemical polarization and impedance measurements using multichannel system Solartron 1470E as electrochemical interface and Solartron 1455A as FRA. The sweep rate of 1 mV/s was used to evaluate the potentiodynamic polarization measurement. The impedance data were conducted over a frequency range from 10 KHz to 10 mHz [19].

3. RESULTS AND DISCUSSION

The x-ray and photographic films are a transparent poly (ethylene terephthalate) plastic coated on one side with a gelatin emulsion containing microscopically small and light-sensitive silver halide crystals. The presence of gelatin in the recycled films beside silver salt directed our aim to use gelatin as reducing and stabilizing agent beside PVP as illustrated in the experimental section to produce high dispersed AgNPs. The scheme of preparation is represented in Scheme 1. In this reaction the AgNPs were prepared using one-step method where nanoparticles were produced directly in the presence of PVP, glucose and NaOH or ammonia solution. The particles agglomerations and size growth of Ag NPS can be prohibited by using PVP and gelatin as reducing and capping agent [21-23]. In this respect, Ag^+ ions were stripped from X-ray films in aqueous solution of sodium hydroxide or ammonia solution, and Ag+ ions were reduced to Ag^0 (Ag NPs) by gelatin and glucose as reducing agents [24]. The present work aims to convert silver chloride (recycled from x-ray waste films) in ammonia or sodium hydroxide solutions without using reducing agent to produce Ag NPs as illustrated in the following equations 1 and 2:

$$AgCl + 2NH_3 \rightarrow Ag(NH_3)_2{}^+ + Cl^- \tag{1}$$

$$2\,AgCl\,(s) + 2\,NH_4OH\,(aq) \rightarrow Ag_2O\,(s) + H_2O\,(l) + 2\,NH_4Cl\,(aq) \tag{2}$$

With more NH_4OH, the brown/black Ag_2O dissolves forming the soluble silver salt. The objective of the work extended to prepare silver nanoparticle having monodisperse particle size below 10 nm with high yield and having strong stability against environment and aqueous acidic solution. The dispersability of Ag NPs can be solved by sing glucose along with PVP and sodium hydroxide as nontoxic reagents. This study aimed to prepare highly dispersed silver nanoparticles with high yield without using external reducing agent which based on toxic amine or using environmentally friendly reducing agent such as glucose. This method is new to reduce silver chloride with gelatin in basic media at low temperature. Gelatin can stabilize Ag NPs surfaces by the amine pendant groups on its backbone with the formation of a steric barrier [25]. The color of stripped silver cation solutions in the presence of gelatin and the absence of glucose were gradually changed from colorless to blue and then to dark red at various temperature.

$$Ag^+ + \tfrac{1}{2}\,C_6H_{12}O_6 + \tfrac{1}{2}H_2O \xrightarrow{\triangle} Ag + \tfrac{1}{2}C_6H_{11}O_7{}^- + \tfrac{3}{2}H^+$$
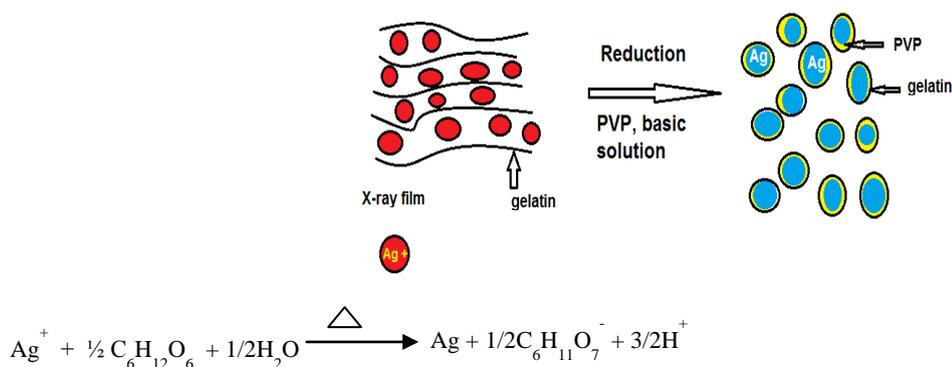
Scheme 1. Synthesis of Ag NPs from x-ray films.

The presence of glucose changes the color of solution from colorless to dark brown and finally to black. The changes of the color indicate the formalization of Ag NPs in both solutions.

The optimum condition to form high yield from Ag NPs such as stripping time, ammonia and sodium hydroxide concentrations, glucose concentration are determined and illustrated in Figure 1 a-d. The data represented that the silver ions stripped after 30 minutes from x-ray films at 50 $^{\circ}$C. This relation was used to optimize the energy used to obtain Ag NPs. Moreover, the optimum concentrations to obtain high yields of Ag NPs are 1 mol/L, 28 wt% and 2 wt % of NaOH, ammonia solution and glucose, respectively as represented in Figure 1 b-d.
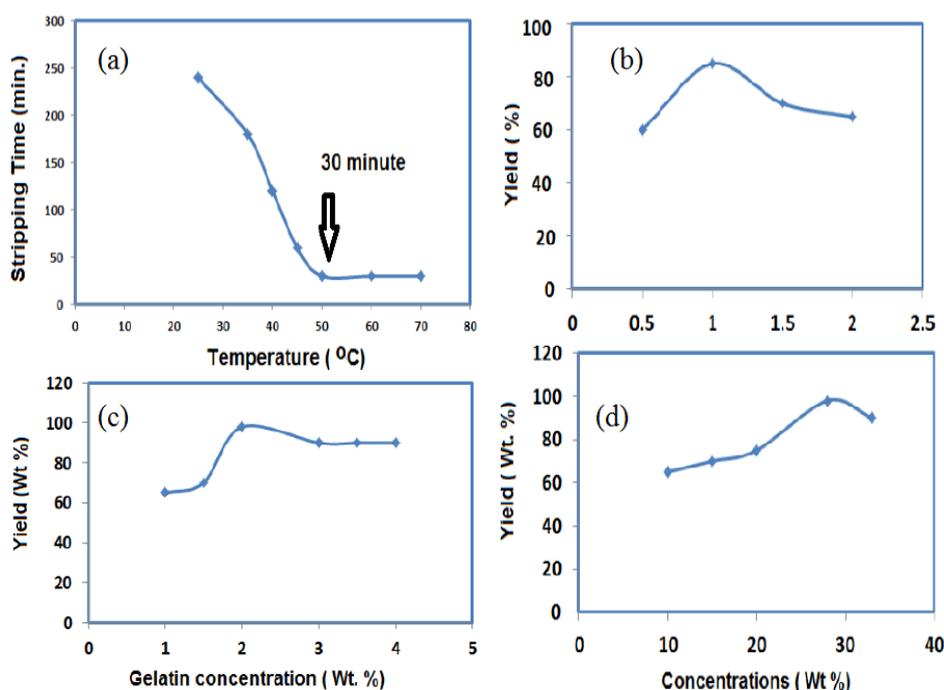
Figure 1. Optimum reaction conditions to obtain Ag NPs.

3.1. Characterization of Ag NPs

The formation of Ag NPs from recycled X-ray films can be elucidated from uv-visible spectroscopy by the appearance of a surface Plasmon resonance (SPR) band at around 400 nm as represented in Figure 2. The data listed in Figure 2 show an interesting characteristic intense sharp peak with red-shift in the λ_{max} of the SPR peak at 400 nm when Ag NPs prepared in the presence of glucose. While the broad band with a shift to left (blue-shift) and low intensity of λ_{max} at 445-400 nm obtained, Figure 2, in the absence of glucose at the same condition as illustrated in the experimental section. The increment of absorbance of peak of Ag NPs/gelatin/ glucose more than Ag NPs formed in absence of glucose indicates the increase of Ag NPs concentration with high yield due to higher reduction of silver ions by glucose [26,27]. Moreover, the sharp red shifts of λ_{max} of Ag NPs/gelatin/ glucose indicates that the size of Ag particles was decreased with the formation of monodisperse Ag NPs than that prepared in the absence of glucose. This observation can be referred to the presence of

glucose and gelatin facilitates the reduction and dissociation of nanoparticles to form smaller particles capped by the amine pendant groups of PVP and gelatin [28].
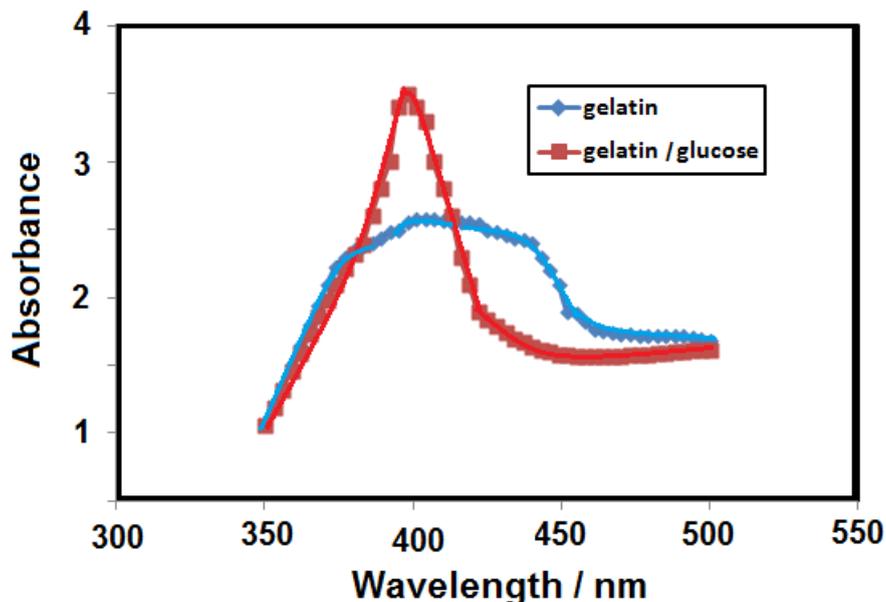
Figure 2. UV-visible Plasmon of the prepared Ag NPs in the presence of gelatin and glucose as capping and reducing agents.

The particle size and dispersability of Ag NPs were determined from Zeta size measurements as represented in Figure 3 a and b. The particle size and polydispersity index (PDI) data, Figure 3, confirm that monodisperse Ag NPs with low diameter 4.2 nm when glucose, NaOH and PVP were used. The data of particle size confirm the data obtained from uv-visible spectroscopy, Figure 2.
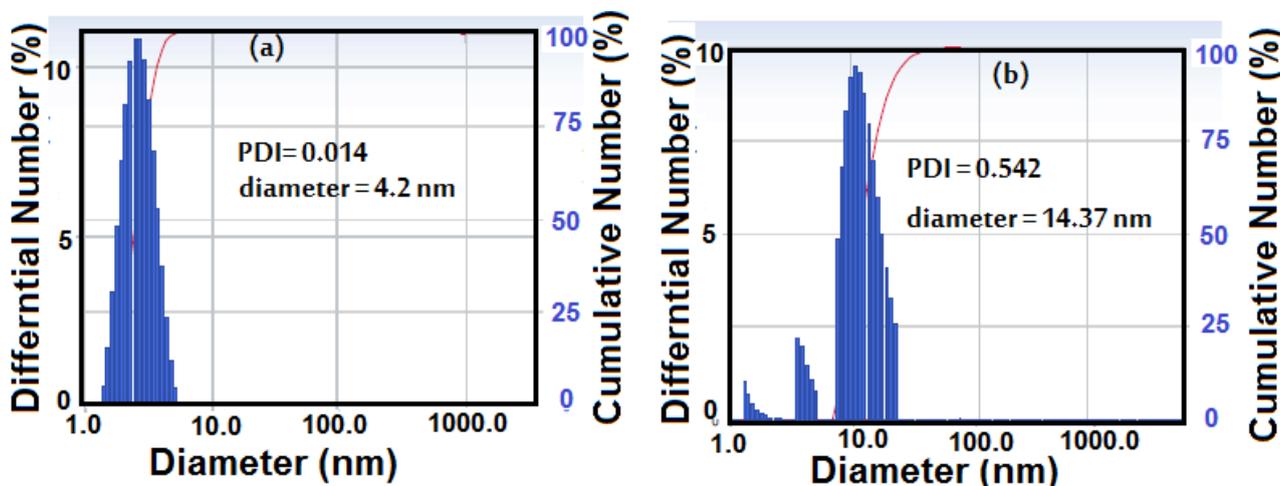
Figure 3. Particle size analysis of Ag NPs prepared a) in the presence of glucose and b) in absence of glucose.

The shape and morphology of Ag NPs are determined from HR-TEM micrographs as represented in Figure 4 a-c. The TEM micrograph of Ag NPs in the presence of glucose solution,

Figure 4 a, retained a small, narrower and uniform particle size distribution which attributed to increased rate of reduction reaction due to glucose presence. The black dots inside the spherical particles can be related to the Ag NPs while the transparent shell can be referred to gelatin and PVP which stabilized silver nanoparticles and increased their dispersability in water. The particle size and shape were decreased to be less than 12 nm, and a smaller particle size (about 3-4 nm) was obtained for Ag NPs prepared in gelatin and PVP solution. The core-shell structure with 4 nm thick of PVP and gelatin was observed in Figure 4 c. The TEM data agree in harmony with uv-visible and Zeta size data.
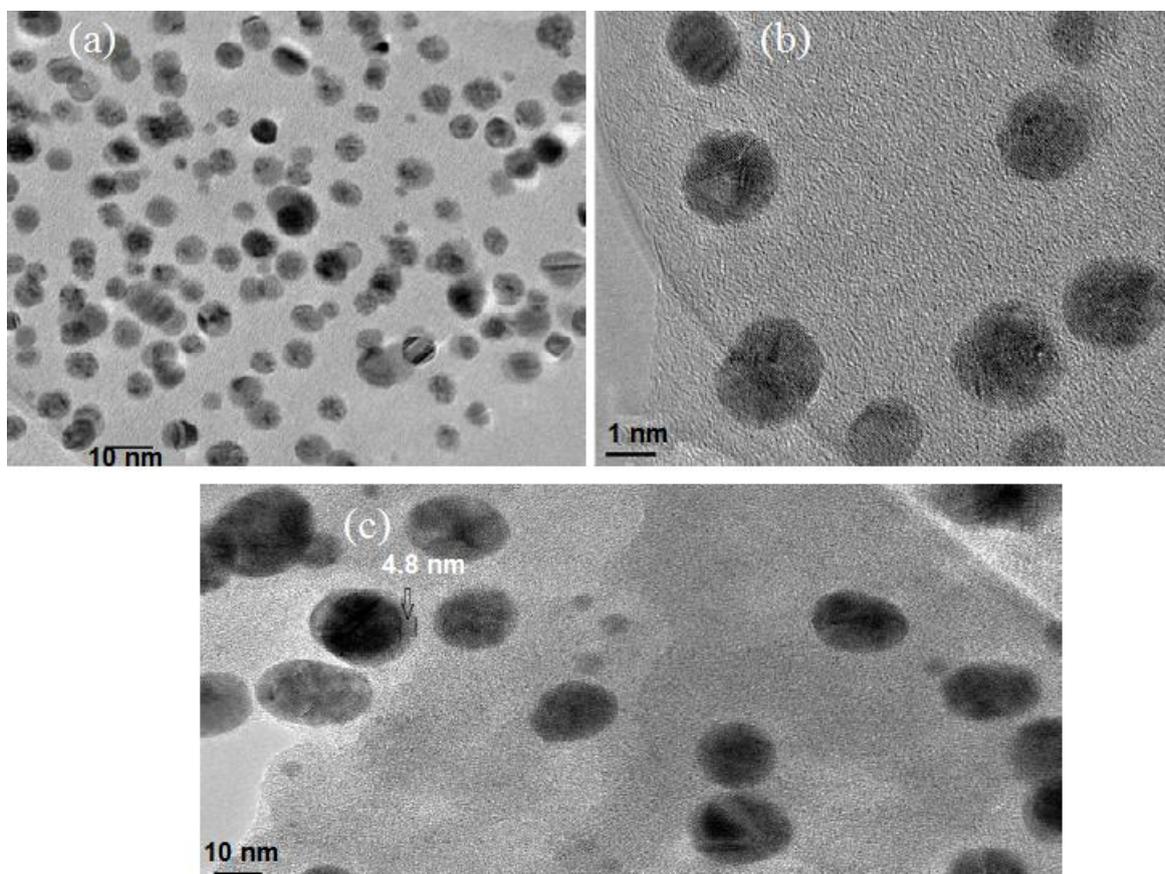
Figure 4. HRTEM micrographs of Ag NPs prepared of a) in the existence of glucose b) in absence of glucose and c) in presence of glucose and PVP.

The AFM also used to show the surface morphology and dispersability of Ag NPs formed from x- ray and photographic films obtained in PVP and in presence or absence of glucose media. Figure 5 a and b showed that the uniform packed monodisperse and dense Ag NPs were formed in the presence of glucose while aggregates were formed in absence of glucose. These data also confirm that the AgNPs prepared in presence and absence of glucose could form biocompatible films which have rough surface to apply for biological uses.
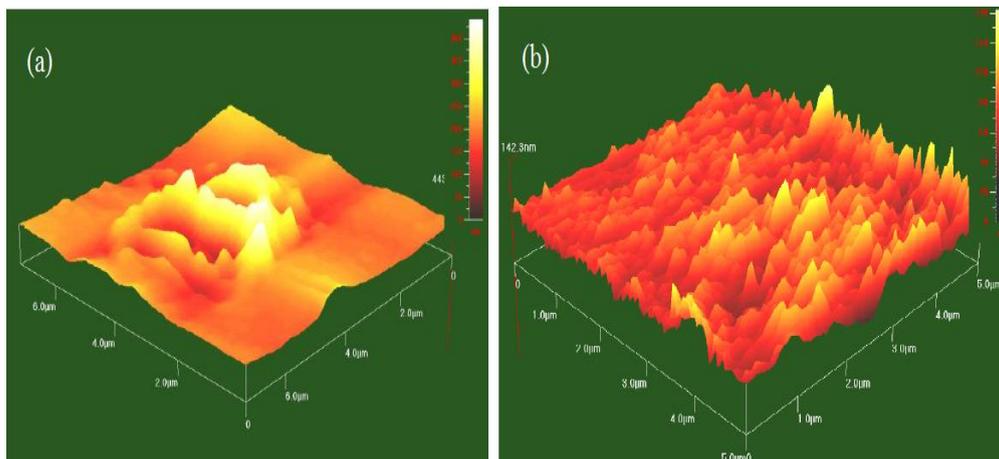
Figure 5. AFM photo of Ag NPs prepared a) in the presence of glucose and b) in absence of glucose.

The formation of pure Ag NPs can be confirmed from XRD spectra. The XRD pattern in Figure 6 a and b shows that the Ag NPs prepared in the presence and absence of glucose consisted of metallic Ag with a cubic structure. The broadening of Ag NPs peaks indicates very small sizes of Ag crystallites. The production of pure Ag NPS without formation of Ag_2O can be confirmed from the appearance of XRD patterns at 2θ of 38.1, 46.3, 64.6, and 77.5^o which referred to the (111), (200), (220), and (311) crystalline planes of face-cantered-cubic silver, respectively (JCPDS file No. 00-004-0783) [29].
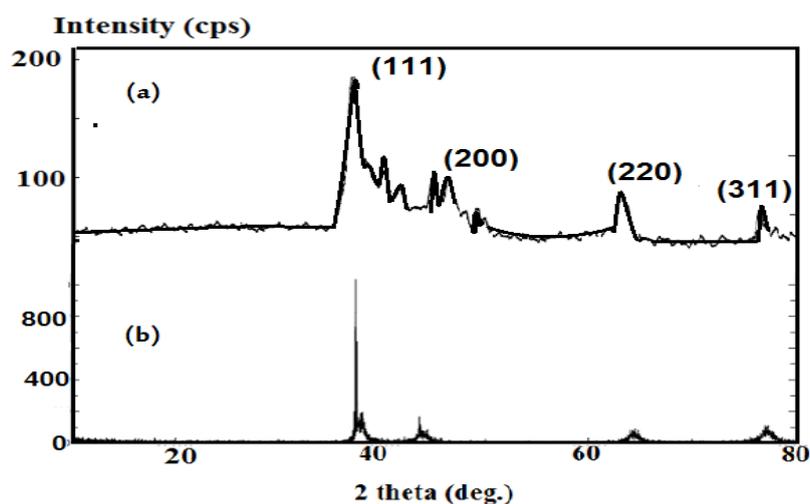
Figure 6. XRD patterns of Ag NPs prepared a) in the presence of glucose and b) in absence of glucose.

3.2. Antimicrobial activity

It is very important to measure the antimicrobial effects of Ag NPs after synthesis by green method to complete the green chemistry rules. Moreover, the effective antimicrobial nanoparticles have been used to inhibit the microbial corrosions beside they incorporated into various medical

applications [30]. It is important to prevent biofilm formation from E. coli, Enterococcus, Staphylococcus aureus, Candida albicans, Staphylococci, and Pseudomonas aeruginosa to measure the significant in vitro antimicrobial activity and toxicity of nanoparticles [31]. It is established that the presence of Ag NPs increase the antibacterial activities of antibiotics for both Gram- positive and Gram-negative bacteria [32]. There are two important parameters used to evaluate the antimicrobial activity such as the minimum bactericidal concentration (MBC; $\mu L\ mL^{-1}$)) which is the minimum concentration of the sample required to achieve irreversible inhibition, i.e., killing bacteria after a defined period of incubation. The second parameter is the minimum inhibition concentration, MIC, which determine the minimum concentration ($\mu L\ mL^{-1}$) of nanoparticles used to inhibit the bacterial growth. MBC and MIC data were determined for both the prepared AgNPs in the presence and absence of glucose using standard dilution micro-method illustrated in the experimental section and listed in Table 1. The dilution micro-method is preferred to estimate the antibacterial performance of Ag NPs diluted two times and up to 128 times. The data listed in Table 1 provide evidence that Ag NPs synthesized using glucose as reducing agent has higher antibacterial activity than those prepared in the absence of glucose. This behavior is correlated to the lower size and higher dispersability of colloidal Ag NPs prepared in presence of glucose than that prepared in absence of it. Moreover, the lowest antimicrobial effect was related not only to the particle size, but also to the rapid formation of aggregates as elucidated from Zeta size analyses (Figure 3 b). The proposed mechanism for antimicrobial activity of Ag NPs based on the release of silver ions to generate reactive oxygen species (ROS) which interact with membrane proteins of bacteria and affect their correct function [33]. The data listed in Table 1 indicates the higher antibacterial sensitivity of Ag NPS towards the Gram-positive S. aureus although the high thickness of peptidoglycan layer of S. aureus which protects the bacteria against antibacterial agents such as antibiotics, toxins, chemicals, and degradative [34- 36]. This means that the silver nanoparticles have great efficiencies to diffuse inside the bacterial membrane. The data listed in Table 1 confirmed also that the tested Ag NPs have bactericidal effects resulting not only in inhibition of bacterial outgrowth but also in killing bacteria as determined from MBC and MIC data.

Table 1. Antimicrobial activity of Ag NPS towards different types of gram- positive and gram-negative bactrai strains.

Antimicrobial materials	Bacteria strain	MBC ($\mu L\ mL^{-1}$)	MIC ($\mu L\ mL^{-1}$)	The reduction of organism (%)			
				0.1 $\mu L\ mL^{-1}$	0.25 $\mu L\ mL^{-1}$	0.5 $\mu L\ mL^{-1}$	5 $\mu L\ mL^{-1}$
Ag NPs	*E. coli*	-	5	54±7	64±8	87±1	95±2
	S. aureus	5	0.5	-	55±7	96±2	100
	B. subtilis	-	0.5	58±4	78±6	90±3	98±0.6
	P. aeruginosa	-	0.5	65±3	77±8	86±4	95±3
Ag NPs in the presence of glucose	*E. coli*	-	10	40±12	55±4	70±7	89±3
	S. aureus	-	1	90±6	94±4	98±1	98±1
	B. subtilis	10	2.5	40±15	97±3	99±0.4	100

3.3. Electrochemical measurements
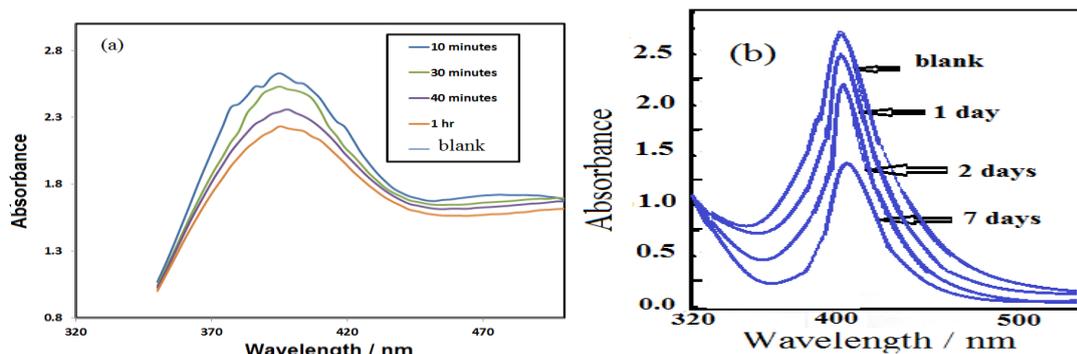
Figure 7. UV- visible spectra of Ag NPs prepared in a) absence of glucose and b) in the presence of glucose using 1 M HCl aqueous solution at different times.

It is well established that silver metal has great stability towards HCl but it is soluble in HCl when the size of silver reduced to nano size [37]. In our previous work, we increased the stability of silver nanoparticle by using a suitable capping agent such as natural products based on Murrh, modified amphiphilic thiol polymers and crosslinked nanogels [38-41]. In the present work the stability of Ag NPs prepared from recycled photographic and x-ray films in the presence and absence of glucose towards 1 M HCl was investigated using UV- visible analysis as illustrated in Figure 7.

The prepared Ag NPs displayed SPR band as represented in uv-visible spectroscopy (Figure a and b). The stability of Ag NPs against 1M HCl was detected from the change of absorbance with time.

The data listed in Figure 7 a indicate that the concentrations of silver nanoparticles prepared in absence of glucose were decreased during 1 h of immersion in 1M HCl. These data elucidated the poor stability of Ag NPs capped with PVP or gelatin in absence of glucose towards 1 M HCl [38]. Moreover, the broadening of peaks indicates the agglomeration of Ag NPs that were easily solubilized in HCl to produce AgCl precipitate. Figure 7 b confirms the high stability of Ag NPs that prepared in the presence of glucose which showed great stability to 1 M HCl for 1 week without aggregations and dissolution. This observation was referred to lower size, high dispersability and the presence of strong capping shell based on PVP and gelatin layer. The high acid stability of Ag NPs prepared in the presence of glucose confirms the measurements of electrochemical characteristics in 1 M HCl.

The electrochemical properties for different concentrations of Ag NPs prepared in the presence of glucose were evaluated from the polarization curves of carbon steel in 1M HCl solution as represented in Figure 8. The inhibition efficiencies for Ag NPs were calculated as [19]:

$$IE(\%) = i^o_{corr} - i_{corr} / i^o_{corr} \qquad (3)$$

where i^o_{corr} and i_{corr} are the corrosion current densities for carbon steel electrode in the uninhibited and inhibited solutions, respectively.

The data of IE% was defined and listed in Table 2. The data of polarization and IE%, Figure 8 and Table 2, confirmed that only 10 ppm of Ag NPs is sufficient to inhibit the corrosion of steel. This data confirmed the ability of nanoparticles to form thin layer film at steel surface. It is also observed from the corrosion data that Tafel lines (Figure 8) were shifted towards more negative and more

positive potentials during the anodic and cathodic processes, when compared to blank curve. This observation confirms that Ag NPs act as a mixed type inhibitor.

Table 2. Electrochemical parameters of steel towards 1M HCl in the presence different concentrations of Ag NPs prepared in the presence of glucose at 25 ^{o}C.

Concentrations (ppm)	Polarization Method					EIS Method		
	Ba (mV)	Bc (mV)	E_{corr} (V)	i_{corr} $\mu A/cm^2$	IE%	R_p Ohm	Cdl ($\mu F/cm^2$)	IE%
Blank	69	120	-0.395	839	_____	1.80	334	_____
5	50	394	-0.306	152	81.8	10.1	137	82.1
10	41	173	-0.313	49	94.1	35	106	94.8
50	46	195	-0.328	44	94.7	36	104	95.0

The Nyquist diagrams of steel in 1 M HCl were used to determine the electrochemical impedance spectroscopy (EIS) as evaluated from equation [42]:

$$Z_{CPE} = 1/A \times 1/(jw)^n \qquad (4)$$

Where A and ω ($\omega = 2\pi f$, where f is the AC frequency) are the CPE constant and the angular frequency, respectively. The imaginary unit (j) and exponent (n) can be used to confirm the heterogeneity and formation of rough surfaces. The inhibition efficiency (IE) can be determined from EIS measurements as:

$$IE\% = (1 - R_{ct} / R^*_{ct}) \times 100 \qquad (5)$$

where R^*_{ct} and R_{ct} are the charge-transfer resistances with and without inhibitors, respectively. The EIS spectra of steel in the absence and presence of Ag NPs were illustrated in Figure 9 and Table 2.
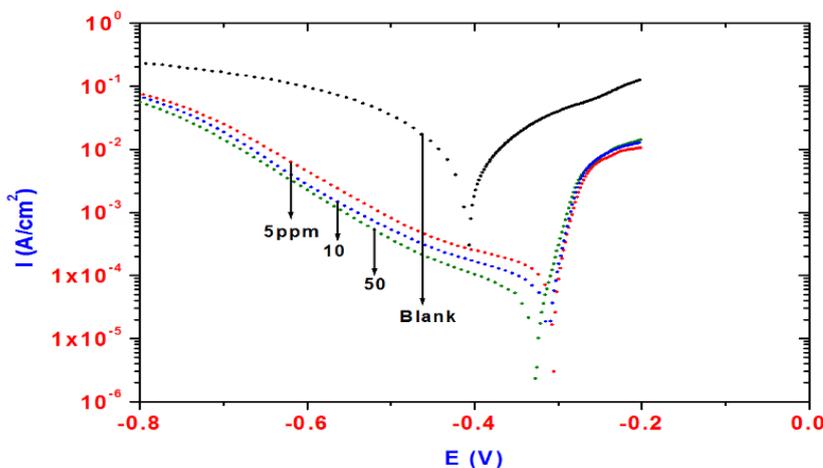
Figure 8. Polarization curves for steel in 1.0 M HCl in the presence of different concentrations of Ag NPs prepared in the presence of glucose.
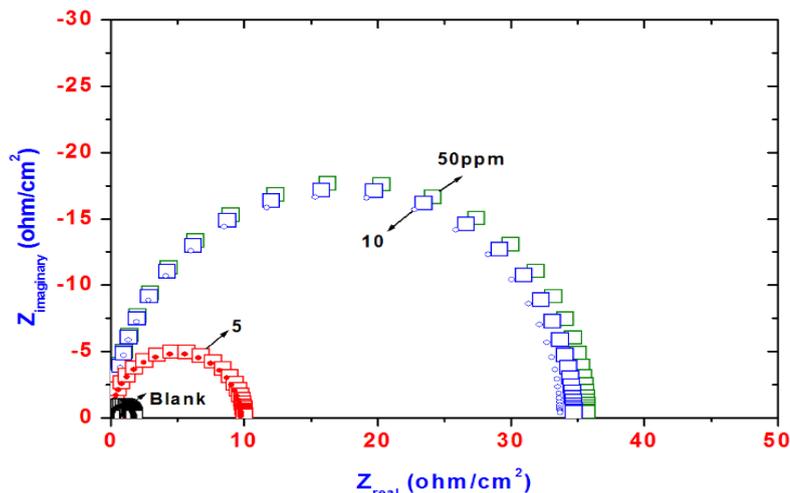
Figure 9. Nyqusit plot for steel in 1.0 M HCl in the presence of different concentrations of Ag NPs prepared in the presence of glucose.

All curves exhibit one single semicircle and the diameter of semicircle increases with the increase of Ag NPs concentration. IE% (table 2) value agrees in harmony with the data obtained from potentiodynamic polarization curves. Moreover, it was observed that the Rct values increased with Ag NPs concentration increment. This means that the steel corrosion is controlled by the charge transfer and the formation of thin layer films of Ag NPs at the steel surfaces [43, 44].

4. CONCLUSIONS AND OUTLOOK

A new green method used to prepare valuable Ag NPs from recycled wastes of medical x-ray and photographic films without using hazardous materials. It was found that the size of Ag NPs was decreased with increasing reaction temperature the up to 60 ^{o}C and as using a reducing agent beside gelatin, which can be related to the rate of reduction reaction. The antimicrobial activity indicates that the prepared Ag NPs increased with the presence of glucose due to their ability to diffuse into the bacterial membrane. The prepared Ag NPs show high stability towards 1 M HCl and form stable thin films on steel surfaces to protect them from corrosion. Finally, it can be concluded that, the green chemistry fundamentals are applied to design, apply new processes to prepare environmentally friendly Ag NPs and eliminate the generation of hazardous substances.

References

1. P. Anastas, and J. Warner, Ph.D. in *Green Chemistry: Theory and Practice* (Oxford University Press: New York, (1998),

2. A. Nagy and G. Mestl, *Appl. Catal. A: Gen.,* 188 (1999) 337–353.
3. A. M. Smith, H. Duan, M. N. Rhyner, G. Ruan and S. Nie, *Phys. Chem. Chem. Phys.,* 8 (2006) 3895–3903.
4. G. J. Kearns, E. W. Foster and J. E. Hutchison, *Anal. Chem.*, 78 (2006) 298–303.
5. V. K. Sharma, R. A. Yngard and Y. Lin, *Adv. Colloid. Interfac.,* 145 (2009) 83–96.
6. G. P. Rao and J. Yang, *Appl. Spectrosc.,* 64 (2010) 1094-1099.
7. R. S. Patil, M. R. Kokate, C. L. Jambhale, S. M. Pawar, S. H. Han and S. S. Kolekar, *Adv. Nat. Sci. Nanosci. Nanotechnol.,* 3 (2012) 7pp.
8. A. Frattini, N. Pellegri, D. Nicastro and O. D. Sanctis, *Mater. Chem. Phys.,* 94 (2005) 148–152.
9. A. Panacek, L. Kvitek, R. Prucek, M. Kolar, R. Vecerova, N. Pizurova, V. K. Sharma and T. Nevecna, R. Zboril, *J. Phys. Chem. B,* 110 (2006) 16248–16253.
10. B. Wiley, Y. Sun and Y. Xia, *Acc. Chem. Res.,* 40 *(*2007) 1067–1076.
11. Q. Yang, F. Wang, K. Tang, C. Wang and Z. Chen, *Mater. Chem. Phys.,* 78 (2003) 495–500.
12. Y. Socol, O. Abramson, A. Gedanken, Y. Meshorer, L. Berenstein and A. Zaban, *Langmuir,* 18 (2002) 4736–4740.
13. J. Zhu, X. Liao and H. Y. Chen, *Mater. Res. Bull.,* 36 (2001) 1687–1692.
14. K. A. Bogle, S. D. Dhole and V. N. Bhorashor, *Nanotechnology***,** 17 (2006) 3204–3208.
15. H. Jia, W. Xu, J. A. Lid and B. Zhao, *Spectrochim. Acta A,* 64 (2006) 956–960.
16. U.U. Jadhav and H. Hocheng, *J. achiev. Mater. Manufact. Eng.,* 54 (2012) 159-163.
17. A. D. Bas, E. Y. Yazici and H. Deveci, *Hydrometallurgy,* 121 (2012) 22–27.
18. Z. Han, J. Wei, M. Zhao and J. Hu, *Hydrometallurgy*, 92 (2008) 148–151.
19. G. A. El-Mahdy, A. M. Atta, and H. A. Al-Lohedan, *J. Taiwan Inst. Chem. Eng.,* 45 (2014) 1947-1953.
20. A. M. Atta, A. M. El-Saeed, G. M. El-Mahdy and H. A. Al-Lohedan, *RSC Adv.,* 5 (2015) 101923-101931.
21. M. Darroudi, M. B. Ahmad, A .K. Zak, R. Zamiri and M. Hakimi, *Int. J. Mol. Sci.,* 12 (2011) 6346-6356.
22. W. J. Jin, H. K. Lee, E. H. Jeong, W. H. Park and J. H. Youk, *Macromol. Rapid Commun.,* 26 (2005) 1903–1907.
23. M. Darroudi, M. B.Ahmad, A. H. Abdullah and N. A. Ibrahim, *Int J Nanomedicine,* 6 (2011) 569-574.
24. R. Janardhanan, M. Karuppaiah, N. Hebalkar and T. N. Rao, *Polyhedron,* 28 (2009) 2522-2530.
25. M. Akbulut, N. K. Reddy, B. Bechtloff, S. Koltzenburg, J. Vermant and R. K. Prud'homme, *Langmuir,* 24 (2008) 9636-9641.
26. M. Darroudi, M. B. Ahmad, K. Shameli, A. H. Abdullah and N. A. Ibrahim, *Solid State Sci.,* 11 (2009) 1621–1624.
27. J. R. Heath, *Phys Rev B*., 40 (1989) 9982–9985.
28. J. J. Zhang, M. M. Gu, T. T. Zheng and J. J. Zhu, *Anal Chem*., 81 (2009) 6641–6648
29. T. Morita, Y. Yasuda, E. Ide, Y. Akada and A. Hirose, *Mater. Trans*., 49 (2008) 2875-2880.
30. Y. Le, P. Hou, J. Wang and J. F. Chen, *Mater. Chem. Phys*., 120 (2010) 351-355.
31. D. Roe, B. Karandikar, N. Bonn-Savage, B. Gibbins and J. B. Roullet. *J. Antimicrob. Chemother.,* 61 (2008) 869-876.
32. A. Kumar, P. K. Vemula, M. Ajayan and G. John, *Nat Mater.,* 7 (2008) 236-241.
33. S. Prabhu and E. K. Poulose, *Int. Nano Lett.,* 2 (2012) 1-10.
34. S. H. Kim, H. S. Lee, D. S. Ryu, S. J. Choi and D. S. Lee, *Korean J. Microbiol. Biotechnol*., 39 (2011)77–85.
35. J. R. Morones, J. L. Elechiguerra, A. Camacho, K. Holt, J. Kouri, J. T. Ramirez and M. J. Yacaman, *Nanotechnology,* 16 (2005) 2346-2353.
36. H. C. Neu, *Science,* 257(1992) 1064-1073.
37. A. M. Atta, G. A. El-Mahdy and H. A. Al-Lohedan, *Int. J. Electrochem. Sci.,* 8 (2013) 4873-4885.

38. A. M. Atta, H. A. Al-Lohedan and A.O. Ezzat, *Molecules*, 19 (2014) 6737-6753.
39. M. S. Alla, H. A. Al-Lohedan and A. M. Atta, *Dig. J. Nanomater. Bios.,* 10 (2015) 253-264.
40. A. M. Atta, H. A. Allohedan, G. A. El-Mahdy and A. O. Ezzat, *J. Nanomater.,* (2013) 132.
41. A. M. Atta, H. A. Allohedan, A. O. Ezzat and Z. A. Issa, *Polym. Sci. Ser. B*, 56 (2014) 762-769.
42. R. Macdonald and D.R. Franceschetti, in: J.R. Macdonald (Ed.), Impedance Spectroscopy, Wiley, New York, (1987) 96-106.
43. X. H. Li, S. D. Deng and H. Fu, *J. App. Electrochem.*, 40 (2010) 1641–1649.
44. L. Larabi, Y. Harek, M. Traianel and A. Mansri, *J. Appl. Electrochem.*, 34 (2004) 833-839.